

Spatiotemporal transmission dynamics of the COVID-19 pandemic and its impact on critical healthcare capacity

Cuadros, D. F., Xiao, Y., Mukandavire, Z., Correa-Agudelo, E., Hernández, A., Kim, H. & MacKinnon, N. J.

Author post-print (accepted) deposited by Coventry University's Repository

Original citation & hyperlink:

Cuadros, DF, Xiao, Y, Mukandavire, Z, Correa-Agudelo, E, Hernández, A, Kim, H & MacKinnon, NJ 2020, 'Spatiotemporal transmission dynamics of the COVID-19 pandemic and its impact on critical healthcare capacity', *Health and Place*, vol. 64, 102404.

<https://dx.doi.org/10.1016/j.healthplace.2020.102404>

DOI 10.1016/j.healthplace.2020.102404

ISSN 1353-8292

Publisher: Elsevier

NOTICE: this is the author's version of a work that was accepted for publication in *Health and Place*. Changes resulting from the publishing process, such as peer review, editing, corrections, structural formatting, and other quality control mechanisms may not be reflected in this document. Changes may have been made to this work since it was submitted for publication. A definitive version was subsequently published in *Health and Place*, 64 (2020) DOI: 10.1016/j.healthplace.2020.102404

© 2020, Elsevier. Licensed under the Creative Commons Attribution-NonCommercial-NoDerivatives 4.0 International <http://creativecommons.org/licenses/by-nc-nd/4.0/>

Copyright © and Moral Rights are retained by the author(s) and/ or other copyright owners. A copy can be downloaded for personal non-commercial research or study, without prior permission or charge. This item cannot be reproduced or quoted extensively from without first obtaining permission in writing from the copyright holder(s). The content must not be changed in any way or sold commercially in any format or medium without the formal permission of the copyright holders.

This document is the author's post-print version, incorporating any revisions agreed during the peer-review process. Some differences between the published version and this version may remain and you are advised to consult the published version if you wish to cite from it.



Spatiotemporal transmission dynamics of the COVID-19 pandemic and its impact on critical healthcare capacity

Diego F. Cuadros^{a,b,c,*}, Yanyu Xiao^{c,d}, Zindoga Mukandavire^{e,f}, Esteban Correa-Agudelo^{a,b,c}, Andrés Hernández^{a,b,c}, Hana Kim^{a,b,c}, Neil J. MacKinnon^{c,g}

^a Department of Geography and Geographic Information Science, University of Cincinnati, Cincinnati, OH, USA

^b Health Geography and Disease Modeling Laboratory, University of Cincinnati, Cincinnati, OH, USA

^c Geospatial Health Advising Group, University of Cincinnati, Cincinnati, OH, USA

^d Department of Mathematical Sciences, University of Cincinnati, Cincinnati, USA

^e Centre for Data Science, Coventry University, UK

^f School of Computing, Electronics and Mathematics, Coventry University, UK

^g James L. Winkle College of Pharmacy, University of Cincinnati, Cincinnati, OH, USA

ARTICLE INFO

Keywords:

COVID-19
Spatially-explicit mathematical model
Transport connectivity
Spatial epidemiology
Critical healthcare capacity

ABSTRACT

The role of geospatial disparities in the dynamics of the COVID-19 pandemic is poorly understood. We developed a spatially-explicit mathematical model to simulate transmission dynamics of COVID-19 disease infection in relation with the uneven distribution of the healthcare capacity in Ohio, U.S. The results showed substantial spatial variation in the spread of the disease, with localized areas showing marked differences in disease attack rates. Higher COVID-19 attack rates experienced in some highly connected and urbanized areas (274 cases per 100,000 people) could substantially impact the critical health care response of these areas regardless of their potentially high healthcare capacity compared to more rural and less connected counterparts (85 cases per 100,000). Accounting for the spatially uneven disease diffusion linked to the geographical distribution of the critical care resources is essential in designing effective prevention and control programmes aimed at reducing the impact of COVID-19 pandemic.

1. Introduction

The coronavirus disease 2019 (COVID-19) pandemic represents a global public health emergency unparalleled in recent history. In the five months since the initial World Health Organization (WHO) reported the COVID-19 outbreak in Wuhan, China, the number of confirmed cases globally has risen sharply from 282 to more than 5,000,000, including 360,000 related deaths. After initial emergence in China, travel-related cases started appearing in other parts of the world with strong travel links to Wuhan (Institut, 2020). The first confirmed case in the U.S. was a travel-related case in Snohomish County, WA, screened on January 19, 2020. In late February, a second presumptive case was identified approximately 10 miles away from where the first case was treated. As of the afternoon of June 7, the U.S. reported 1,920,904 confirmed COVID-19 cases, and 109,901 confirmed COVID-19 deaths (University, 2019).

In the early stages of a new infectious disease outbreak, it is crucial to

understand the transmission dynamics of infection (Kucharski et al., 2020). Recognizing the temporal and spatial dynamics of the infection can provide insights into the epidemiological characteristics of the disease and identification of disease hotspots. Spatiotemporal analysis can inform forecasting of the potential future burden of the disease, help identify drivers of local transmission and populations at higher risk, and guide the designing of targeted interventions in resource limited settings (Wilson and Halperin, 2008; Meyer-Rath et al., 2018). In the context of the novel COVID-19, most studies have focused in understanding the temporal dynamics of COVID-19 to produce temporal trajectories of the disease under different populations and intervention scenarios (Kucharski et al., 2020; Prem et al., 2020; Hellewell et al., 2020; Ayoub et al., 2020a; Mukandavire et al., 2020), with some few studies assessing the spatio-temporal dynamics of the disease (Huang et al., 2020; Gatto et al., 2020; Jia et al., 2020).

To date, the role of geospatial disparities in shaping disease transmission dynamics is poorly understood. Infectious diseases, including

* Corresponding author. Department of Geography and Geographic Information Science, University of Cincinnati, Cincinnati, OH, 45221, USA.

E-mail address: diego.cuadros@uc.edu (D.F. Cuadros).

<https://doi.org/10.1016/j.healthplace.2020.102404>

Received 11 June 2020; Received in revised form 15 July 2020; Accepted 20 July 2020

Available online 25 July 2020

1353-8292/© 2020 The Authors.

Published by Elsevier Ltd.

This is an open access article under the CC BY-NC-ND license

(<http://creativecommons.org/licenses/by-nc-nd/4.0/>).

respiratory infections, have substantial geographical variation in intensity and range of transmission induced by uneven distribution of vulnerable populations and risk factors that facilitate (or hamper) the spatial diffusion of the pathogen (Green et al., 2016; Caini et al., 2018; Park et al., 2020; Real and Biek, 2007; Sloan et al., 2011). This is of high relevance considering the unequal distribution of the capacity of the healthcare system, which might strongly determine disease outcomes (Ji et al., 2020). Regions across the U.S have not been equally affected by the COVID-19 pandemic, with the Northeastern part of the country reporting more cases and deaths (van Dorn et al., 2020). The underlying causes of these regional differences in the country are currently not well understood. Preliminary studies have identified socioeconomic (e.g. higher population of ethnic minorities), health-related (e.g. comorbidities with chronic diseases), and environmental factors such as air pollution, as key drivers of geographical disparities of COVID-19 related hospitalizations and deaths (van Dorn et al., 2020; Wu et al., 2020; COVID, 2020). In a previous study we found that the spatial distribution of these factors along with other spatial attributes such as airport and road connectivity were linked to the geospatial disparities of COVID-19 related risk of mortality in the U.S (Correa-Agudelo et al., 2020).

Understanding the local variation in disease transmission dynamics under heterogeneous geospatial attributes is a crucial step in developing more effective strategies for mitigating risk of infection in vulnerable communities. Therefore, in this study, we built a spatially-explicit mathematical model to predict the county-level spatial dynamics of COVID-19 epidemic in a region. The model was calibrated using data from the state of Ohio in the U.S. Ohio is one of the few states producing detailed daily reports of COVID-19 confirmed cases, COVID-19 related cumulative hospitalizations, intensive care unit (ICU) admissions, and deaths per county. Likewise, Ohio is a state with marked variation of demographic and geographic attributes among counties along with substantial differences in the capacity of healthcare within the state. Our aim is to predict the spatiotemporal dynamics of the COVID-19 pandemic in relation with the distribution of the capacity of healthcare in Ohio.

2. Methods

2.1. Mathematical model

We developed a spatial mathematical model to simulate the transmission dynamics of COVID-19 disease infection and spread. The spatially-explicit model incorporates geographic connectivity information at county level. The Susceptible-Infected-Hospitalized-Recovered-Dead (SIHRD) COVID-19 model classified the population into susceptibles (S), confirmed infections (I), hospitalized and ICU admitted (H), recovered (R) and dead (D). Based on a previous study that identified local air hubs and main roads as important geospatial attributes linked to differential COVID-19 related hospitalizations and mortality (Correa-Agudelo et al., 2020; Cuadros et al., 2020), we stratified the SIHRD COVID-19 model into four different spatial risk groups based on defined connectivity index for each county. The spatial risk groups were defined as follows, Group 1: *counties with airports with more than 50,000 passengers per year*; Group 2: *counties surrounding the counties with airports*; Group 3: *counties with main highways crossing the county*; and Group 4: *counties not surrounding counties with airports or being crossed by main highways*. The dynamics of disease transmission and infection progression in each group were modeled using seven epidemiological compartments for the SIHRD COVID-19 model (Fig. S1). Susceptible individuals in each spatial group were at risk of being exposed to infection at varying hazard rates, which are group- and time dependent, to capture the variability in the risk of exposure and the impact of public health interventions. A detailed description of the model is given in the *Supplementary Materials*.

2.2. Model fitting and parameterization

We used data from the Ohio Department of Health (Health ODo, 2020). The model was fitted using the following data sets: 1) cumulative number of confirmed COVID-19 cases, 2) cumulative number of COVID-19-related hospitalizations, 3) cumulative number of ICU admissions, and 4) cumulative number of COVID-19 deaths in each county in Ohio from March 5 to May 10, 2020. We used an out-of-sample model validation approach to test the performance of the model. We withheld 20% of the data and conducted model fitting and parameterization using data from March 1 to April 25 as the estimation period, and data from April 26 to May 10 were used as the validation period to assess the accuracy of model estimates (Fig. S2). Since we were interested in simulating COVID-19 transmission dynamics in the general population, we excluded data from Marion and Pickaway counties, which experienced unusual confined and explosive COVID-19 outbreaks. Marion Correctional Institution is the site of one of the biggest COVID-19 outbreaks in Ohio, driving the Marion County to the highest rate of COVID-19 cases in the state. Pickaway County experienced a similar situation with a surge of a COVID-19 outbreak in a prison, becoming the second confined hotspot in Ohio after Marion prison. We used model fitting to estimate the hazard rate in each spatial risk group, rate of infection flow from other spatial risk groups, hospitalization rate, discharge rate from hospitals, ICU admission rate, recovery rate from ICU admission, and death rate in each spatial risk group. The model included the impact of public health interventions such as social distancing and stay home order implemented in Ohio that changed the transmission dynamics of the disease at a specific time point. We used a nonlinear least-square data fitting method, based on the Nelder-Mead simplex algorithm (Lagarias et al., 1998) to minimize the sum of squares between data points and model predictions. We conducted a multivariable uncertainty analysis to determine the range of uncertainty around model predictions. We performed 10,000 simulation runs using a Latin Hypercube sampling from a multidimensional distribution of the model parameters, in which parameter values were selected from ranges specified by assuming $\pm 30\%$ uncertainty around parameters' point estimates (Ayoub et al., 2020a, 2020b), and the resulting distributions of estimates across all runs were used to calculate the 95% Credible Intervals (CrIs) of model estimations. Analyses were performed in MATLAB R2017a (MATLAB, 2017).

2.3. Model scenarios

We first assessed the impact of geospatial attributes (transport connectivity) in the local dynamics of the pandemic. We created two types of maps: 1) spatially adjusted maps were generated using the projections from each spatial risk group to estimate the number of confirmed COVID-19 cases in each county, depending on the county classification in each spatial risk group and the proportion of the total population of the risk group residing in the county; and 2) for the non-spatially adjusted maps, the projections from each spatial risk group were combined to generate a single model estimation for the cumulative number of COVID-19 cases for Ohio, and these COVID-19 cases estimates were distributed depending to the proportion of the total population from Ohio residing in the county.

In the second scenario, we used the model to generate projections of the impact of potential easing on the non-pharmaceutical interventions in the critical care capacity of each county in Ohio. We assessed the impact of 50% reduction on the estimated impact of non-pharmaceutical interventions in reducing the hazard rate of infection. Under this scenario we calculated the proportion of ICU beds occupied by COVID-19 patients in each county one week, five weeks, and eight weeks after the easing of the social distancing intervention. We used data from the Definitive Healthcare database (Definitive Healthcare, 2020) to estimate the number of available ICU beds under normal circumstances in each county (Fig. S3). We estimated the ratio of ICU beds occupied by

COVID-19 patients over the total number of ICU beds available in each county at one week, five weeks and eight weeks after the easing of social distancing intervention and also assuming a baseline scenario of maintaining the status quo of the current social distancing interventions implemented in Ohio. Results were displayed in maps created using ArcGIS® by ESRI version 10.5 (<http://www.esri.com>) (ESRI, 2004).

3. Results

The model estimated a total number of 21,430 (95% CrI 18,965–31,754) COVID-19 cases compared to the 20,763 confirmed cases (excluding Marion and Pickaway counties) reported by May 10, 2020 in Ohio. Likewise, the model estimated 4,318 (95% CrI 3,807–5,937) cumulative hospitalizations, 1,362 (95% CrI 1,185–1,825) cumulative ICU admissions, and 1,529 (95% CrI 1,314–2,120) cumulative COVID-19 related deaths compared to 4,054 hospitalizations, 1,205 ICU admissions, and 1,421 deaths reported by May 10, 2020 in Ohio (Fig. 1).

We found substantial variations in the spread and intensity of the infection among the different spatial risk groups. The epidemic was spreading faster and affecting more individuals in counties with local air hubs from Group 1, whereas the rural and less connected counties from Group 4 experienced a slower and less severe spread of the disease (Fig. 2). The infection rate of COVID-19 was almost three times higher in Group 1, with an average of 274 cases per 100,000 people, compared to an average of 85 cases per 100,000 people in the rural and less connected counties from Group 4, with a hazard rate of infection in this group three-fold smaller relative to Group 1 (Fig. 2). Similarly,

cumulative COVID-19 related hospitalizations were twice higher in counties with local air hubs, with an average of 48 hospitalizations per 100,000 people, compared to an average of 23 hospitalizations per 100,000 people in the less connected counties from Group 4.

Estimations generated using the non-spatial adjusted model over-estimated COVID-19 infection rate in the rural and less connected counties from Group 4, estimating an average of 185 cases per 100,000 inhabitants, compared to the actual number of 85 cases per 100,000 people in these counties. Conversely, this model underestimated the infection rate in the local air hub counties (Group 1), with 176 cases per 100,000 inhabitants, compared to the actual number of 247 cases per 100,000 people in these counties (Fig. 3).

Critical healthcare capacity measured as ICU beds available shows substantial disparities among counties in Ohio (Fig. S2). Highly populated and connected counties with local air hubs from Group 1 had the highest critical healthcare capacity, with 22 ICU beds available per 100,000 people, whereas the rural and less connected counties from Group 4 had, on average, nine ICU beds available per 100,000 people. Disease projections using the spatial model indicated that assuming a 50% easing of social distancing intervention, air hub counties would reach 94% of the maximum ICU bed capacity in eight weeks after the intervention is relaxed. Conversely, the rural and less connected counties from Group 4 would reach 55% of the maximum ICU bed capacity eight weeks after the intervention is relaxed (Fig. 4). Critical care capacity would remain stable at 27% of the maximum capacity if no changes in the intervention are introduced.

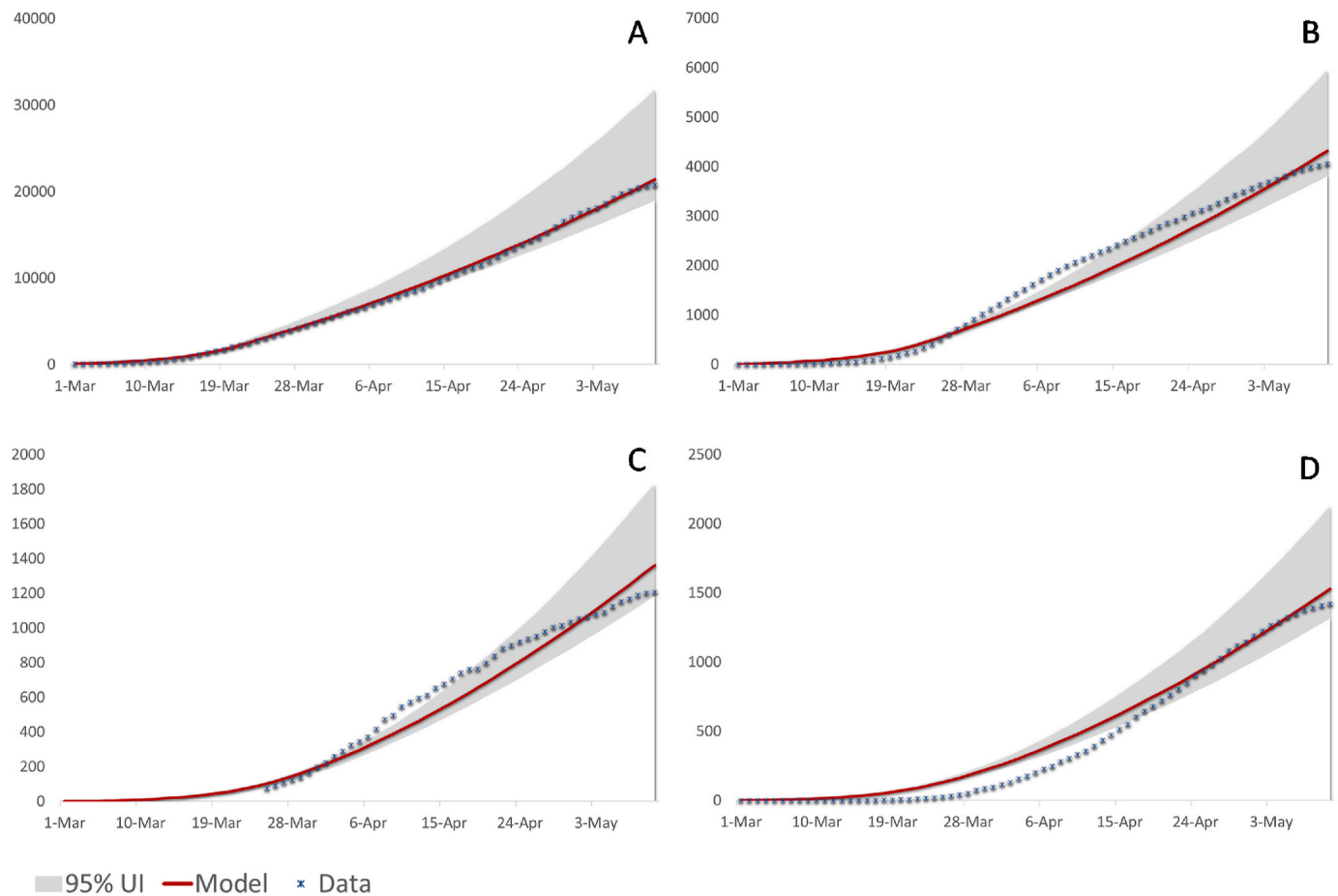


Fig. 1. Temporal dynamics of the cumulative number of COVID-19 cases (A), hospitalizations (B), ICU admissions (C), and deaths (D). Red lines illustrate model estimations, with their corresponding 95% credible interval (grey areas). Blue marks illustrate data values. (For interpretation of the references to color in this figure legend, the reader is referred to the Web version of this article.)

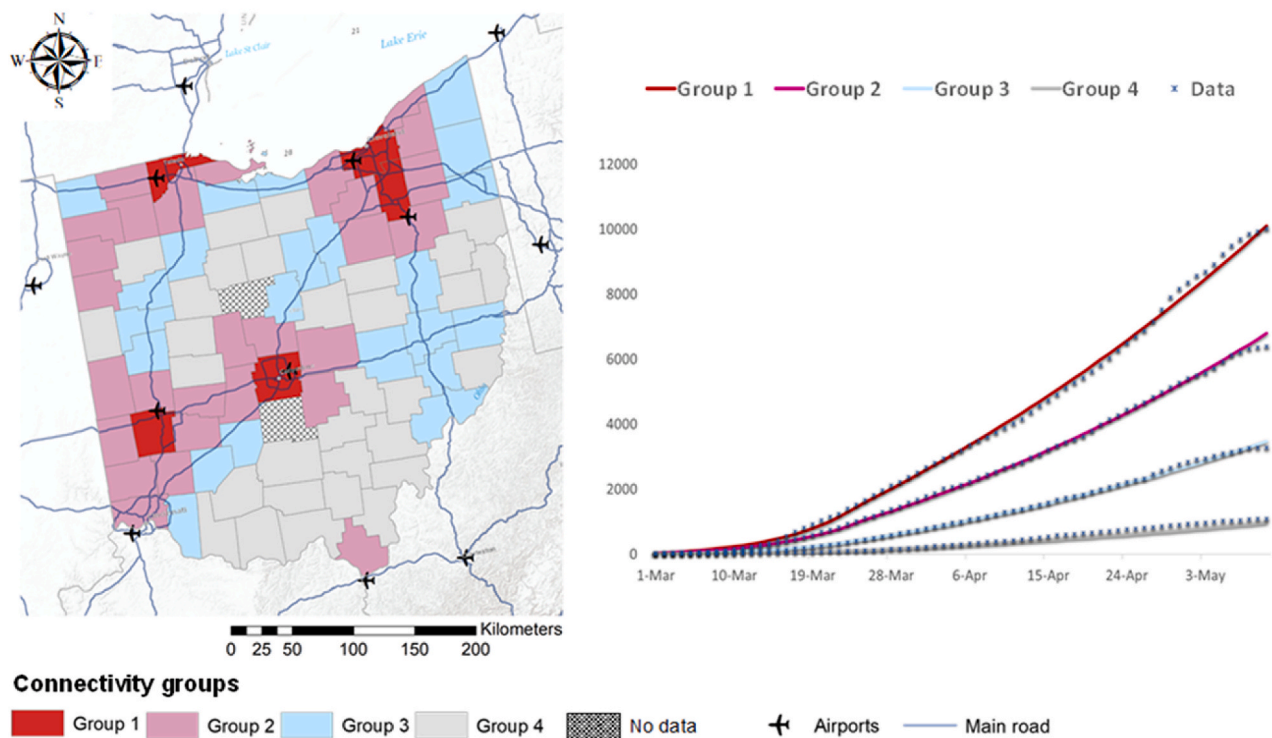


Fig. 2. Map in the left illustrates the distribution of the counties in the different spatial risk groups, counties in Group 1 are illustrated on red color, Group 2 in dark pink, Group 3 in blue, and Group 4 in grey. Figure in the right illustrate the temporal dynamics of the cumulative number of COVID-19 confirmed cases in each of the different spatial risk groups. Maps were created using ArcGIS® by ESRI version 10.5 (<http://www.esri.com>) (ESRI, 2004). (For interpretation of the references to color in this figure legend, the reader is referred to the Web version of this article.)

4. Discussion

We assessed the geospatial variation of the spread of the novel SARS-CoV-2 virus in Ohio, U.S., and the impact of the differential spatiotemporal dynamics of the disease in the uneven critical healthcare capacity of the state. The results showed substantial geographical variation in the dynamics of the disease with some local areas experiencing much faster and intensive spread of the infection compared to other areas. Counties in which the connectivity is enhanced by air transportation had faster spread of infection compared to nearby counties, counties with high road connectivity, and more isolated rural counties in Ohio. The non-spatial adjusted model showed that these geographical differences in the severity of the COVID-19 epidemic among counties were not only generated by the uneven distribution of the population in the state but also by underlying spatial attributes like transport connectivity that might introduce substantial variation in the local dynamics of the infection.

More than 47% of the confirmed COVID-19 cases in Ohio were concentrated in only five counties included in Group 1 (Cuyahoga, Franklin, Lucas, Montgomery and Summit), with an average infection rate of 274 cases per 100,000 people. These counties are characterized by a high population density, with 35% of the total population of the state residing in these five counties, but they are also local air hubs with airports that receive more than 10,000,000 passengers every year. The high connectivity and travelers in these counties generated by airports can produce a high influx of locally imported infections that boost the local transmission of the virus in the county and consequently accelerate the spread of the infection in these areas (Organization, 2020; Warren et al., 2010). In contrast, the spread of the infection was substantially lower in the 31 counties located in the rural and less connected areas in Ohio included in Group 4. Although these less densely populated counties are home of only 11% of the total population in Ohio, the

infection rate was more than three times lower compared to the infection rate in the local air hub counties.

We also identified marked differences in the geographical distribution of the critical healthcare capacity of the state. More than 50% of the total number of ICU beds available are in the five counties included in Group 1 with a rate of 22 ICU beds per 100,000 people. In contrast, only 7% of the total number of ICU beds available in the state are distributed in the 31 counties located in the rural and less connected areas of the state, with a rate of 10 ICU beds per 100,000 people. Despite these local differences in the critical healthcare capacity of the state, our modeling results suggest that the differential local dynamics of the disease, with substantially less transmission in these rural and less connected counties, prevented the saturation of the critical care response in these areas. We found that if the non-pharmaceutical interventions implemented in the state in mid-March 2020 were maintained after early May, only 27% of the maximum critical care capacity of the state would be reached, and along with the 10 counties that do not have hospitals with ICU beds. Three more counties, Clermont, Delaware, and Lawrence would reach more than 50% of their maximum critical care capacity under this scenario. In contrast, our predictions indicated that if the intervention is eased by 50%, an estimated 61% of the maximum critical healthcare capacity of the state would be reached eight weeks after the relaxation of the intervention. However, areas with more intense transmission of the disease (Group 1) would experience a faster saturation of the critical care capacity. Although these counties had the highest critical healthcare capacity, the faster and more intense spread of the epidemic experienced in these areas would substantially impact the critical care response in these counties. As a result, the healthcare capacity in these counties would be almost completely saturated (94% of the maximum capacity) eight weeks after the social distancing intervention is eased. Conversely, the slower spread of the infection in the rural and less connected counties included in Group 4, which had

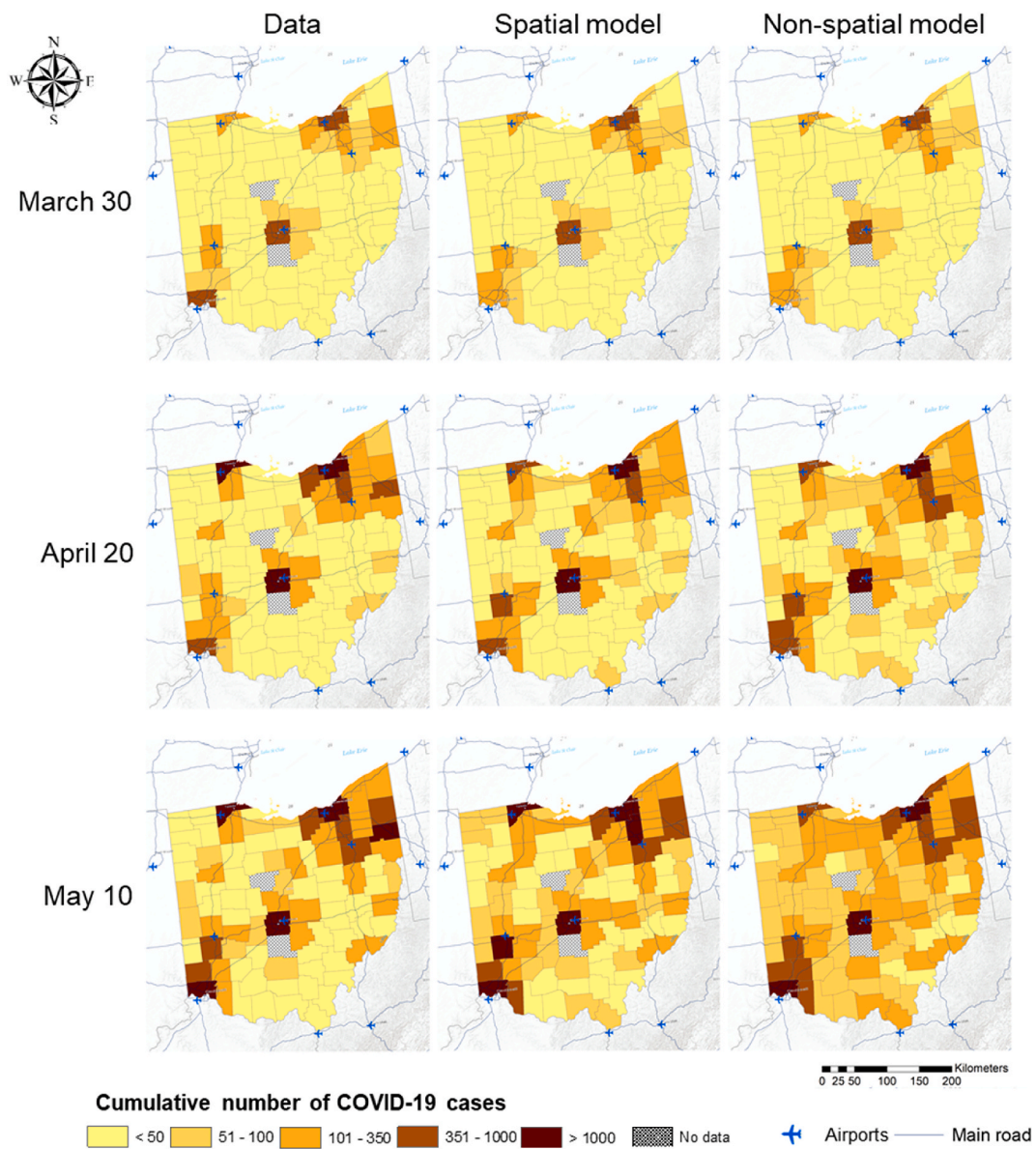


Fig. 3. Spatiotemporal dynamics of the cumulative number of COVID-19 cases estimated from the spatial adjusted and non-spatial adjusted models. Maps were created using ArcGIS® by ESRI version 10.5 (<http://www.esri.com>) (ESRI, 2004).

substantially lower critical care response compared to the counties in Group 1, reduces the possibility of a potential saturation of the critical care response in these areas, and only 55% of the maximum critical healthcare capacity of these counties would be reached eight weeks after social distancing intervention is eased. Noteworthy, eight of the 31 counties from Group 4 do not own hospitals with ICU beds, and counties such as Adams, Champaign, and Seneca would reach more than 60% of their maximum critical care capacity. Therefore, these low connected counties along with the local air hub counties were identified as high priority areas for strategies aimed to strengthen the critical care response against the COVID-19 pandemic in Ohio.

Our study has several limitations worth noting. For simplification, we generated a connectivity index based only in one geospatial attribute in which airports and main roads were used as a connectivity index for each county. Other potential geospatial and population characteristics might influence transmission dynamics and improve estimated disease trajectories, but inclusion of these factors can substantially increase model complexity. Moreover, as noted in the methods section, since we were interested in patterns of infection dynamics in the general

population, we did not include data from Marion and Pickaway counties, which were counties that experienced explosive confined COVID-19 outbreaks occurring in different prisons. However, confined outbreaks could become an important element in the spread of the disease and could have significant impacts in the local critical care capacity in areas they occur. Furthermore, the SIHRD COVID-19 model described here was parameterized using data from the state of Ohio only. The COVID-19 pandemic is composed by series of sub-epidemics of different intensities, even within countries. COVID-19 outbreaks have emerged in different locations at different time periods in the U.S. (Desjardins et al., 2020; Hohl et al., 2020), and each state in the country had implemented different control measures at different times, which might generate substantial differences in the dynamics of the disease. For this reason, it would be important to assess model performance using data from other locations.

Despite these limitations, this study presents one of the first spatiotemporal models of COVID-19 transmission to simulate the spatial disparities in disease outcomes such as the number of confirmed COVID-19 cases, cumulative number of hospitalizations, ICU admissions and

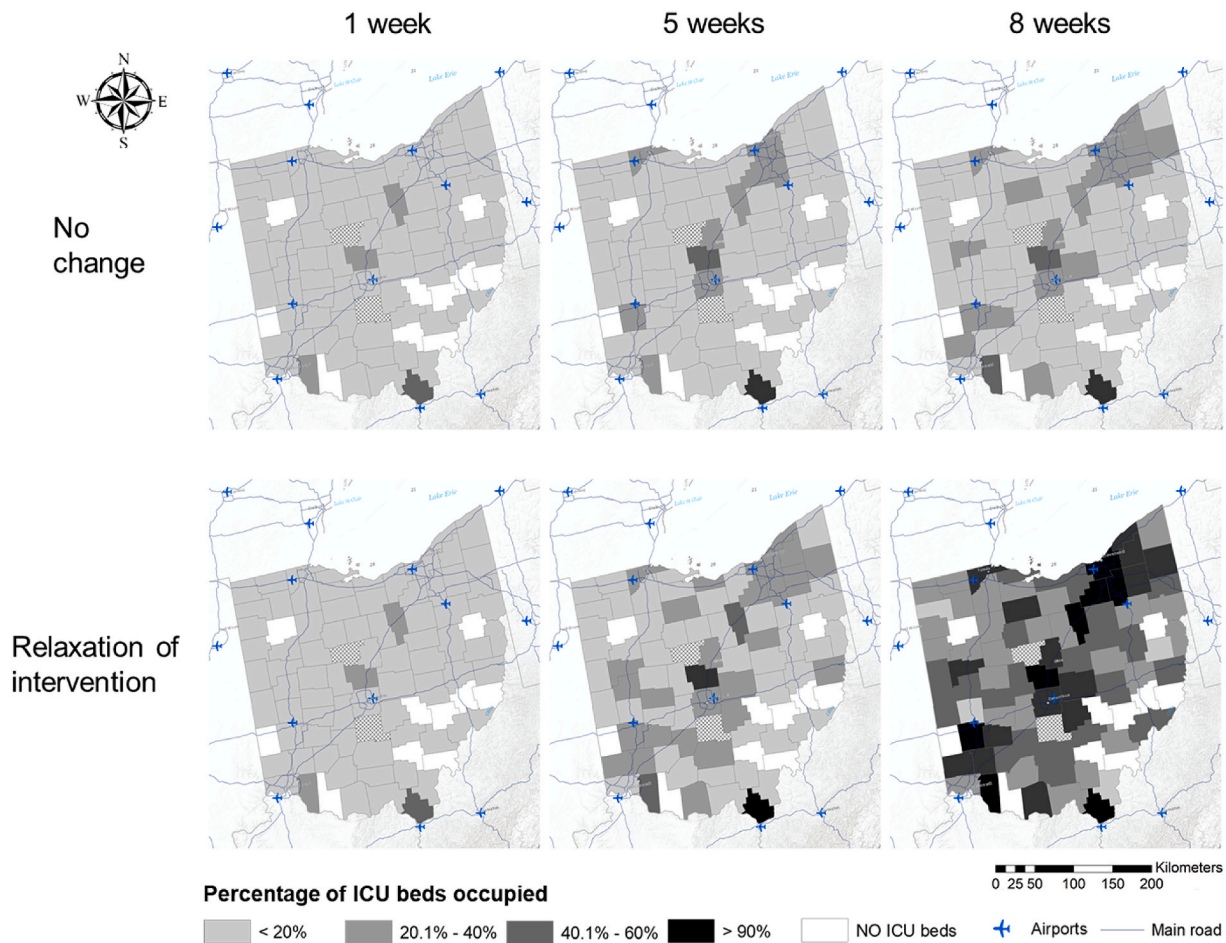


Fig. 4. Spatiotemporal dynamics of the projected proportion of ICU beds occupied under different scenarios of relaxation of the non-pharmaceutical interventions in Ohio. Maps were created using ArcGIS® by ESRI version 10.3 (<http://www.esri.com>) (ESRI, 2004).

deaths on a finer resolution. Using this model, we found substantial spatial variation in the spread of the disease, with localized areas showing marked differences in disease transmission intensity. These dynamic differences in disease transmission are induced not only by the uneven distribution of the population but also by spatial attributes such as the level of air and road connectivity in these areas. As a result, not all local areas are going to reach their maximum critical care capacity at the same time, and failure in the inclusion of geospatial attributes to understand the local disease dynamics can generate inaccurate estimations that are critical, also considering the uneven spatial distribution of the critical healthcare capacity in a region. Higher disease transmission intensity experienced in some highly connected and urbanized areas could substantially impact the critical care response of these areas regardless of their potentially high healthcare capacity compared to their more rural and less connected counterparts (Hall et al., 2006; Hartley, 2004). Therefore, accounting for the spatially uneven disease diffusion linked to the geographical distribution of the critical care resources is key in developing effective prevention and control programmes to contain COVID-19 pandemic (Graves, 2008; Yamashita and Kunkel, 2010). This is particularly important, in view of a potential scenario in which intermittent lockdowns could become a future public health strategy to reduce challenges in the critical healthcare response for future pandemics.

Author statement

All authors have seen and approved the final version of the manuscript being submitted.

Funding source declaration

No funding sources to declare.

Declaration of competing interest

The authors declare no conflict of interest.

Appendix A. Supplementary data

Supplementary data to this article can be found online at <https://doi.org/10.1016/j.healthplace.2020.102404>.

References

- Ayoub, H.H., Chemaitelly, H., Mumtaz, G.R., Seedat, S., Awad, S.F., Makhoul, M., Abu-Raddad, L.J., 2020a. Characterizing key attributes of the epidemiology of COVID-19 in China: model-based estimations. medRxiv. 2020. <https://doi.org/10.1101/2020.04.08.20058214>.
- Ayoub, H.H., Chemaitelly, H., Kouyoumjian, S.P., Abu-Raddad, L.J., 2020b. Characterizing the historical role of parenteral antischistosomal therapy in hepatitis C virus transmission in Egypt. *Int. J. Epidemiol.*
- Caini, S., El-Guerche Séblain, C., Ciblak, M.A., Paget, J., 2018. Epidemiology of seasonal influenza in the middle east and north africa regions, 2010-2016: circulating influenza A and B viruses and spatial timing of epidemics. *Influenza Other Respir. Vir.* 12 (3), 344–352.
- Correa-Agudelo, E., Mersha, T., Hernandez, A., Branscum, A.J., MacKinnon, N.J., Cuadros, D.F., 2020. Identification of Vulnerable Populations and Areas at Higher Risk of COVID-19 Related Mortality in the U.S. medRxiv, 2020.2007.2011.20151563.

- COVID, C., 2020. Response Team. Geographic differences in covid-19 cases, deaths, and incidence-United States, February 12-April 7, 2020. *MMWR Morb. Mortal. Wkly. Rep.* 69 (15), 465–471.
- Cuadros, Diego, MacKinnon, Neil, Xiao, Yanyu, Hernandez, Andres, Correa, Esteban, Kim, Hana, Yao, Zhiyuan, Mavi, Rajinder, Hincapie, Ana, 2020. Identification of Vulnerable Areas of High COVID-19 Mortality Risk in Ohio (Press release). University of Cincinnati, 05/21/2020.
- Definitive Healthcare, L., 2020. Definitive healthcare: USA hospital beds. [https://coronavirus-disasterresponse.hub.arcgis.com/datasets/1044bb19da8d4dbfb6a96eb1b4ebf629_0?geometry=84.902%2C-16.820%2C-109.864%2C72.123&selectedAttribute=ADULT ICU BEDS](https://coronavirus-disasterresponse.hub.arcgis.com/datasets/1044bb19da8d4dbfb6a96eb1b4ebf629_0?geometry=84.902%2C-16.820%2C-109.864%2C72.123&selectedAttribute=ADULT%20ICU%20BEDS). Accessed 05/10/2020.
- Desjardins, M., Hohl, A., Delmelle, E., 2020. Rapid surveillance of COVID-19 in the United States using a prospective space-time scan statistic: detecting and evaluating emerging clusters. *Appl. Geogr.* 102202.
- 2004 ESRI, . ESRI. ArcGIS 10.X. ESRI, Redlands, CA, USA.
- Gatto, M., Bertuzzo, E., Mari, L., et al., 2020. Spread and dynamics of the COVID-19 epidemic in Italy: effects of emergency containment measures. *Proc. Natl. Acad. Sci. Unit. States Am.* 117 (19), 10484–10491.
- Graves, B.A., 2008. Integrative literature review: a review of literature related to geographical information systems, healthcare access, and health outcomes. In: *Perspectives in Health Information Management/AHIMA*, vol. 5. American Health Information Management Association.
- Green, C.A., Yeates, D., Goldacre, A., et al., 2016. Admission to hospital for bronchiolitis in England: trends over five decades, geographical variation and association with perinatal characteristics and subsequent asthma. *Arch. Dis. Child.* 101 (2), 140–146.
- Hall, S.A., Kaufman, J.S., Ricketts, T.C., 2006. Defining urban and rural areas in US epidemiologic studies. *J. Urban Health* 83 (2), 162–175.
- Hartley, D., 2004. Rural health disparities, population health, and rural culture. *Am. J. Publ. Health* 94 (10), 1675–1678.
- Health Odo. COVID-19 dashboard. <https://coronavirus.ohio.gov/wps/portal/gov/covid-19/dashboards/overview>. Accessed 05/10/2020, 2020.
- Hellewell, J., Abbott, S., Gimma, A., et al., 2020. Feasibility of controlling COVID-19 outbreaks by isolation of cases and contacts. *Lancet Glob. Health.*
- Hohl, A., Delmelle, E., Desjardins, M., Lan, Y., 2020. Daily surveillance of COVID-19 using the prospective space-time scan statistic in the United States. *Spatial Spatio-temporal Epidemiol.* 100354.
- Huang, R., Liu, M., Ding, Y., 2020. Spatial-temporal distribution of COVID-19 in China and its prediction: a data-driven modeling analysis. *J. Infect. Dev. Ctries.* 14, 246–253, 03.
- Institut, R.K., 2020. Event horizon - COVID-19. Accessed. (Accessed 26 May 2020).
- Ji, Y., Ma, Z., Peppelenbosch, M.P., Pan, Q., 2020. Potential association between COVID-19 mortality and health-care resource availability. *Lancet Glob. Health* 8 (4), e480.
- Jia, J.S., Lu, X., Yuan, Y., Xu, G., Jia, J., Christakis, N.A., 2020. Population flow drives spatio-temporal distribution of COVID-19 in China. *Nature* 1–5.
- Kucharski, A.J., Russell, T.W., Diamond, C., et al., 2020. Early dynamics of transmission and control of COVID-19: a mathematical modelling study. *Lancet Infect. Dis.*
- Lagarias, J.C., Reeds, J.A., Wright, M.H., Wright, P.E., 1998. Convergence properties of the Nelder–Mead simplex method in low dimensions. *SIAM J. Optim.* 9 (1), 112–147.
- Meyer-Rath, G., McGillen, J.B., Cuadros, D.F., et al., 2018. Targeting the right interventions to the right people and places: the role of geospatial analysis in HIV program planning. *AIDS (London, England)* 32 (8), 957.
- Mukandavire, Z., Nyabadza, F., Malunguza, N., Cuadros, D., Shiri, T., Musuka, G., 2020. Quantifying early COVID-19 outbreak transmission in South Africa and exploring vaccine efficacy scenarios. *PloS One* (in press).
- Organization, W.H., 2020. Management of Ill Travellers at Points of Entry–International Airports, Seaports and Ground Crossings–In the Context of COVID-19 Outbreak: Interim Guidance. World Health Organization, 16 February 2020.
- Park, M., Cook, A.R., Lim, J.T., Sun, Y., Dickens, B.L., 2020. A systematic review of COVID-19 epidemiology based on current evidence. *J. Clin. Med.* 9 (4), 967.
- Prem, K., Liu, Y., Russell, T.W., et al., 2020. The effect of control strategies to reduce social mixing on outcomes of the COVID-19 epidemic in Wuhan, China: a modelling study. *Lancet Publ. Health.*
- Real, L.A., Biek, R., 2007. Spatial dynamics and genetics of infectious diseases on heterogeneous landscapes. *J. R. Soc. Interface* 4 (16), 935–948.
- Sloan, C., Moore, M.L., Harter, T., 2011. Impact of pollution, climate, and sociodemographic factors on spatiotemporal dynamics of seasonal respiratory viruses. *Clin. Transl. Sci.* 4 (1), 48–54.
- MATLAB, 2017. The Language of Technical Computing computer Program.
- University, J.H., 2019. Novel coronavirus COVID-19 (2019-nCoV) data repository by Johns hopkins CSSE. <https://github.com/CSSEGISandData/COVID-19>. Accessed 06/07/2020, 2020.
- van Dorn, A., Cooney, R.E., Sabin, M.L., 2020. COVID-19 exacerbating inequalities in the US. *Lancet* 395 (10232), 1243–1244.
- Warren, A., Bell, M., Budd, L., 2010. Airports, localities and disease: representations of global travel during the H1N1 pandemic. *Health Place* 16 (4), 727–735.
- Wilson, D., Halperin, D.T., 2008. “Know your epidemic, know your response”: a useful approach, if we get it right. *Lancet* 372 (9637), 423–426.
- Wu, X., Nethery, R.C., Sabath, B.M., Braun, D., Dominici, F., 2020. Exposure to Air Pollution and COVID-19 Mortality in the United States. *medRxiv*.
- Yamashita, T., Kunkel, S.R., 2010. The association between heart disease mortality and geographic access to hospitals: county level comparisons in Ohio, USA. *Soc. Sci. Med.* 70 (8), 1211–1218.